

RESEARCH

Open Access



Human arm joints reconstruction algorithm in rehabilitation therapies assisted by end-effector robotic devices

Arturo Bertomeu-Motos^{1*} , Andrea Blanco¹, Francisco J. Badesa², Juan A. Barrios¹, Loredana Zollo³ and Nicolas Garcia-Aracil¹

Abstract

Background: End-effector robots are commonly used in robot-assisted neuro-rehabilitation therapies for upper limbs where the patient's hand can be easily attached to a splint. Nevertheless, they are not able to estimate and control the kinematic configuration of the upper limb during the therapy. However, the Range of Motion (ROM) together with the clinical assessment scales offers a comprehensive assessment to the therapist. Our aim is to present a robust and stable kinematic reconstruction algorithm to accurately measure the upper limb joints using only an accelerometer placed onto the upper arm.

Methods: The proposed algorithm is based on the inverse of the augmented Jacobian as the algorithm (Papaleo, et al., Med Biol Eng Comput 53(9):815–28, 2015). However, the estimation of the elbow joint location is performed through the computation of the rotation measured by the accelerometer during the arm movement, making the algorithm more robust against shoulder movements. Furthermore, we present a method to compute the initial configuration of the upper limb necessary to start the integration method, a protocol to manually measure the upper arm and forearm lengths, and a shoulder position estimation. An optoelectronic system was used to test the accuracy of the proposed algorithm whilst healthy subjects were performing upper limb movements holding the end effector of the seven Degrees of Freedom (DoF) robot. In addition, the previous and the proposed algorithms were studied during a neuro-rehabilitation therapy assisted by the 'PUPArm' planar robot with three post-stroke patients.

Results: The proposed algorithm reports a Root Mean Square Error (RMSE) of 2.13cm in the elbow joint location and 1.89cm in the wrist joint location with high correlation. These errors lead to a RMSE about 3.5 degrees (mean of the seven joints) with high correlation in all the joints with respect to the real upper limb acquired through the optoelectronic system. Then, the estimation of the upper limb joints through both algorithms reveal an instability on the previous when shoulder movement appear due to the inevitable trunk compensation in post-stroke patients.

Conclusions: The proposed algorithm is able to accurately estimate the human upper limb joints during a neuro-rehabilitation therapy assisted by end-effector robots. In addition, the implemented protocol can be followed in a clinical environment without optoelectronic systems using only one accelerometer attached in the upper arm. Thus, the ROM can be perfectly determined and could become an objective assessment parameter for a comprehensive assessment.

Keywords: Neuro-rehabilitation therapy, End-effector robots, Kinematic reconstruction, Upper limbs

*Correspondence: abertomeu@umh.es

¹Miguel Hernández University of Elche, Av. Universidad w/n, Ed. Innova, 03202 Elche, Spain

Full list of author information is available at the end of the article

Background

Robot-assisted therapies have become a new tool in post-stroke upper limb treatments [1, 2]. One of the most common consequences of stroke, brain cells damage caused by an interruption of the blood flow to the brain, is the hemiparesis, a loss of physical strength on one side of the body, as well as memory problems that they directly affect the realization of the Activities of Daily Living (ADL) [3]. The main goal in these kind of therapies is the effective use of neuroplasticity of the brain performing several exercises assisted by a robotic device which can be adapted to the tasks regarding his/her residual motor capabilities. This technology aims to maximize the patient's recovery, minimize the rehabilitation period and encourage the motivation of patients [4–6].

Rehabilitation robotic devices for upper limbs can be classified into two types: exoskeletons devices [7], have robot axes aligned with the anatomical axes of the upper limb segments providing direct control of individual joints, and end-effector devices [8], work by applying mechanical forces to the distal segments of limbs (see Fig. 1). Though exoskeletons allow the total control of the arm joints, they are difficult to adapt and attach to the patient arm [9, 10]. Moreover, the attachment process takes a long time in order to avoid misalignment between the robot and the arm that can injure the patient. However, end-effector robots can be easily adapted and used by several patients with different pathologies [11–14]. Nevertheless, these robots provide information about the end effector trajectory followed during the therapy and the interaction forces between the hand and the end effector, by which the therapist can perform an objective assessment and customize the therapy based on patients' needs [15–17], but they are not able to know the upper limb joints of the patient.

On the other hand, monitoring joint angles enables human posture to be analyzed in a wide range of application and disciplines, such as physical and neuro-rehabilitation, sports medicine or virtual training. The Range of Motion (ROM) in upper limb neuro-rehabilitation therapy offers a comprehensive assessment

together with the clinical assessment scales [18–20]. Standard motion analysis instruments are widely used in these fields that can be mainly divided into three groups: optoelectronic systems, inertial measurement units (IMUs) systems, and wearable goniometers. The former system is often very expensive and difficult to adapt into a clinic environment, it requires a large and controlled area without camera obstruction [21]. The latter is an emerging technology that aims to measure the angle joints by the deformation of a specific sensor or by optical-based goniometers [22–24]. However, they are able to measure only simple joints as a flexo-extension of the knee or the elbow, not a combination of upper limb joints. The IMUs systems, based on the integration of accelerometers, gyroscopes and magnetometers, have gained the reputation of being the cutting edge of wearable motion tracking systems [25, 26]. IMUs estimate the orientation of the body segments where they are attached by combining multi-sensor information through dedicated optimal sensor fusion algorithms. However, the calibration of these sensors is sometimes very difficult to achieve with post-stroke patient due to a specific body configuration requirements, as with the well known XSens MVN system [27], or the system need a fusion of many sensors placed onto the body [28].

There are several studies which have produced arm reconstruction through motion tracking cameras to estimate the position of the arm and implement a visual feedback on rehabilitation activities [29, 30]. However, they do not perform an accurate measurement of the arm joints during the rehabilitation therapy. A new tool capable to compute the arm joints through two non-invasive accelerometers placed onto the upper arm was introduced by Mihelj [31]. Papaleo et al. improved this method by integrating the joint kinematic reconstruction through the inverse of the augmented Jacobian being able to accurately estimate the human upper limb joints using only one accelerometer [32]. Although this algorithm presents a low error with respect to the real arm, it is unstable when a small shoulder movement is done due to the inevitable trunk compensation performed by patients. Furthermore,

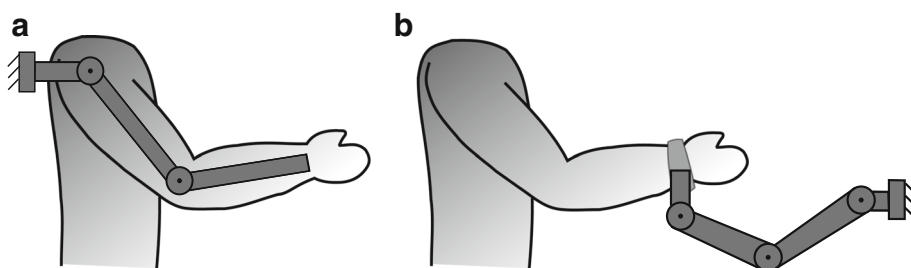


Fig. 1 Robotic devices for upper limb rehabilitation: **a** Exoskeletons, **b** End effector

the system uses the information of an optoelectronic system to measure the upper arm and forearm lengths, the shoulder position, and the initial position.

In this paper, an upper limb kinematic reconstruction algorithm, based on the same criterion presented in [32], is developed. It uses the information provided by one accelerometer placed onto the upper arm and by the end effector of the robot. This algorithm solves the instability in the upper limb joints estimation, proposing a protocol to manually measure the upper arm and forearm lengths and we present a technique to estimate the initial upper limb joints. The main difference between the proposed and the previous algorithm is that the estimation of the elbow joint location is done through computation of the accelerometer rotation after an arm displacement. The end-effector robot with seven Degrees of Freedom (DoF), designed and built by the Neuro-Bioengineering Research Group (nBio), Miguel Hernández University of Elche, Spain, was used to carry out the experimental validation of the proposed algorithm [33]. Furthermore, a comparative analysis of both algorithms in a neuro-rehabilitation therapy with post-stroke patients is performed, studying their behavior when shoulder movements cannot be avoided by patients but measured through the method proposed in [34] using the 'PUPArm' robot.

Methods

Kinematic model of the human arm

The human arm is a complex kinematic chain that can be simplified into seven DoF arm model, connected through

two links: upper arm (l_u) and forearm (l_f), as can be seen in Fig. 2a) [35]. The shoulder has been modeled as a spherical joint composed of abduction-adduction (q_1), flexion-extension (q_2) and internal-external rotation (q_3) movements. The double-hinge elbow joint comprises the flexion-extension (q_4) and pronation-supination (q_5) of the forearm. Though q_5 anatomically belongs to the elbow joint, it is considered as a wrist DoF. Thereby, the wrist joint is a spherical joint composed of q_6 , ulnar-radial deviation (q_6) and flexion-extension (q_7) of the hand. The Denavit-Hartenberg (DH) parameters [36] of the arm and the reference systems of each joint were established as are shown in Table 1 and in Fig. 2b, respectively.

Inverse kinematics with augmented Jacobian

The kinematic reconstruction algorithm is based on the augmented Jacobian introduced by Kreutz-Delgado [37]. The analysis of a seven DoF manipulator with revolute joints was performed to uniquely determine the joint angles for a given end-effector location. The redundancy is catheterized by the swivel angle (α), the angle between the arm plane formed by the shoulder, elbow and wrist points and a reference plane SVW , shown in Fig. 3.

Then, the augmented Jacobian can be expressed as

$$J_A(\vec{q}) = \begin{bmatrix} J_g(\vec{q}) \\ J_\alpha(\vec{q}) \end{bmatrix},$$

where $J_g(\vec{q})$ is the geometric Jacobian matrix of the arm and $J_\alpha(\vec{q})$ is the swivel angle Jacobian, providing the joint velocities with respect to the amount of change of α . Thus,

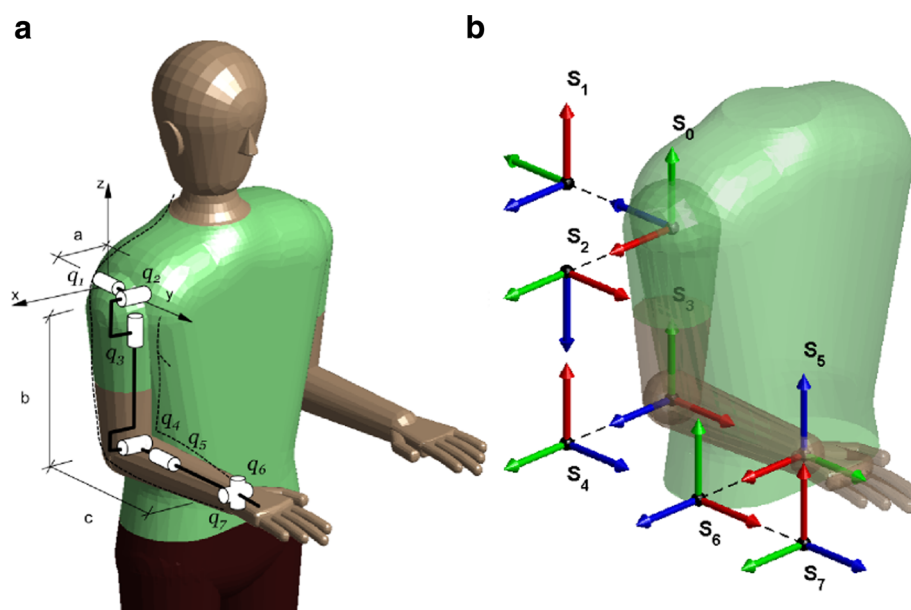


Fig. 2 Simplified human arm model. **a** Rotational joints. **b** DH reference systems where X, Y and Z axes are represented by the red, green and blue colors, respectively

Table 1 DH Parameters of the human arm

| <i>i</i> | θ_i | d_i | a_i | α_i |
|----------|----------------|-------|-------|------------|
| 1 | $\pi/2 + q_1$ | 0 | 0 | $\pi/2$ |
| 2 | $3\pi/2 + q_2$ | 0 | 0 | $\pi/2$ |
| 3 | q_3 | l_u | 0 | $-\pi/2$ |
| 4 | $\pi/2 + q_4$ | 0 | 0 | $\pi/2$ |
| 5 | $\pi/2 + q_5$ | l_f | 0 | $\pi/2$ |
| 6 | $\pi/2 + q_6$ | 0 | 0 | $\pi/2$ |
| 7 | $\pi/2 + q_7$ | 0 | 0 | $\pi/2$ |

the arm joint velocities are computed through the inverse of the augmented Jacobian with respect to the upper limb joints (\vec{q}) as

$$\dot{\vec{q}} = J_A^{-1}(\vec{q}) \left\{ \begin{bmatrix} \dot{\vec{v}}_d \\ \dot{\alpha} \end{bmatrix} + K \cdot \vec{err} \right\}, \quad (1)$$

being $\dot{\vec{v}}_d$ the hand velocity vector and $\dot{\alpha}$ the swivel angle velocity. The error produced by the discrete integration is

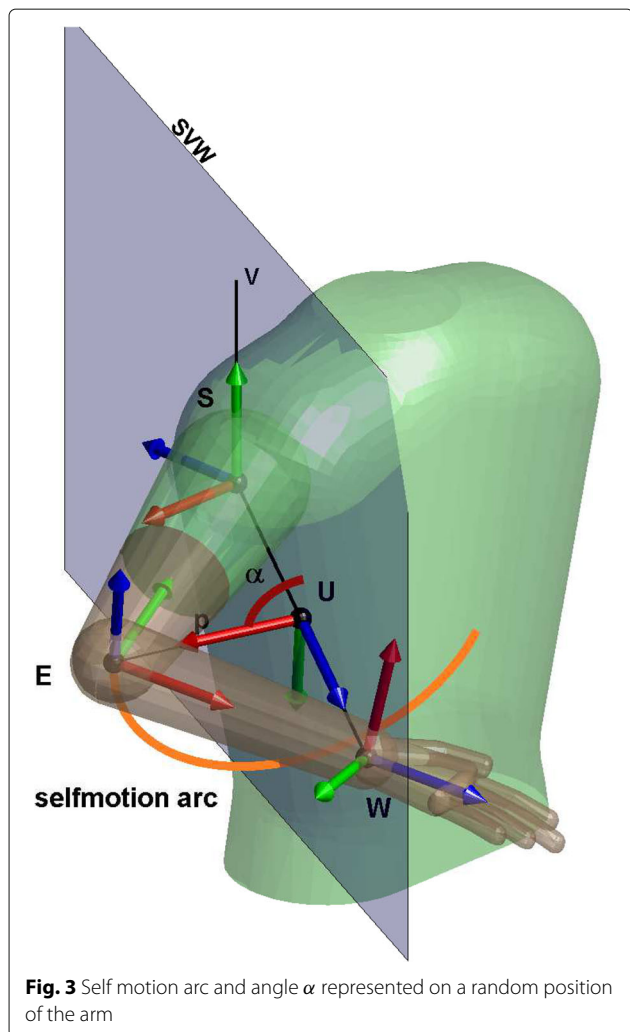


Fig. 3 Self motion arc and angle α represented on a random position of the arm

minimized with the vector error (\vec{err}) multiplied by a suitable gain matrix K [38]. The Jacobian matrix can induce high joint speed in the regions close to kinematic chain singularities. Thereby, the damped least-square approach [38] was applied to the augmented Jacobian matrix as

$$J_A^* = J_A^T (J_A \cdot J_A^T + k^2 \cdot I)^{-1},$$

where k^2 is the damping factor that, chosen properly, performs an accuracy approach to the singularity area, and I is the identity matrix. Therefore, the Jacobian matrix J_A^* is introduced in (1) instead of J_A .

Thus, the arm joints at time t_k are estimated as

$$\vec{q}(t_k) = \vec{q}(t_{k-1}) + \dot{\vec{q}}(t_k) \Delta t,$$

being $\vec{q}(t_{k-1})$ the previous arm joints, $\dot{\vec{q}}$ computed from (1) and Δt the sampling rate.

Elbow estimation

The estimation of the elbow joint pose is the key of the proposed inverse kinematic reconstruction. It is computed through the orientation of the accelerometer placed onto the upper arm. This orientation can be estimated assuming slow movements during the exercise, to erase the dynamic component of the acceleration.

Starting from the reference position of the arm and the accelerometer, shown in Fig. 4, the value of the accelerometer at this position, normalized with respect to the gravity acceleration, is

$${}^{acc}V_g = \begin{bmatrix} 0 \\ 1 \\ 0 \end{bmatrix}.$$

The acceleration value in a random upper limb position can be expressed as a combination of the reference value and the rotation applied (${}^{acc}R_{acc}$) as

$${}^{acc}V_g = ({}^{acc}R_{acc})^{-1} {}^{acc}V_g.$$

The rotation matrix ${}^{acc}R_{acc}$ is unknown, however one possible solution might be computed as

$${}^{acc}\tilde{R}_{acc} = I + M + M^2 \frac{1 - \cos(\theta)}{\sin^2(\theta)},$$

with

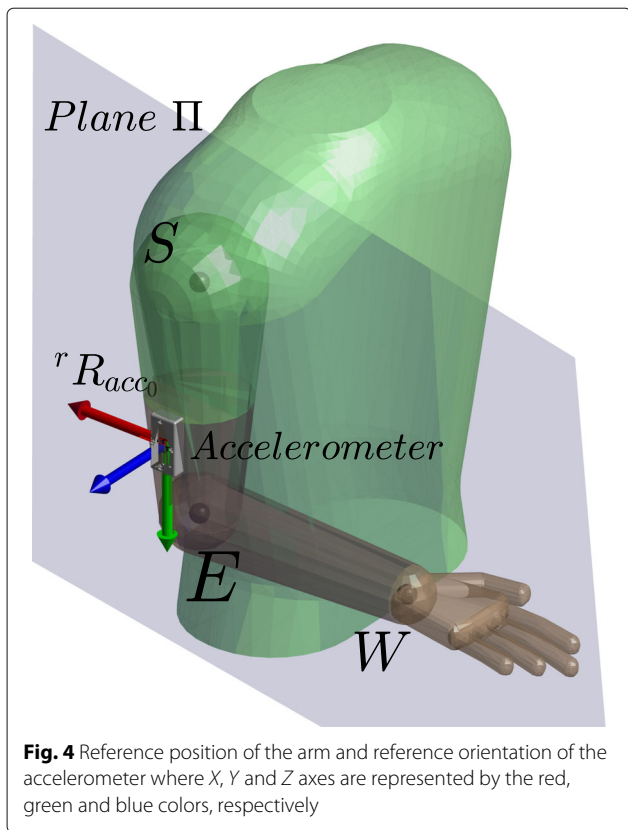
$$M = \begin{bmatrix} 0 & -V(3) & V(2) \\ V(3) & 0 & -V(1) \\ -V(2) & V(1) & 0 \end{bmatrix},$$

$$V = {}^{acc}V_g \times {}^{acc}V_g,$$

$$\sin(\theta) = \|V\|,$$

$$\cos(\theta) = {}^{acc}V_g \cdot {}^{acc}V_g.$$

From this rotation, it is possible to find the proper arm position making the plane XY of ${}^{acc}\tilde{R}_{acc}$ to include the known shoulder and wrist joints position, shown as Π



plane in Fig. 4. Hence, it is necessary to rotate the matrix ${}^{acc0}\tilde{R}_{acc}$ around the gravity vector a γ angle to accomplish this restriction. The computation of this angle is explained in the Additional file 1. The simplification performed in order to obtain this angle allows the algorithm to be performed in real time (average time in the computation of the mathematical operations: $\approx 0.9\text{ ms}$ running on the Intel Core i7 3.40GHz with Matlab R2017a).

Two solutions of angle γ are found, each solution computes a different rotation matrix ${}^{acc0}R_{acc}^{(i)}$, with $i \in \{1, 2\}$, in which the Z axis point to each normal vector of the plane Π . Thus, two elbow positions with respect to the robot ($'P_e$) are obtained as

$$'P_e = {}^r T_{acc} \cdot [0 \ lu \ 0 \ 1]^T, \text{ with}$$

$$'T_{acc} = \begin{bmatrix} {}^r R_{acc0} \cdot {}^{acc0}R_{acc}^{(i)} & {}^r P_s \\ 0 & 1 \end{bmatrix},$$

being $'T_{acc}$ the homogeneous matrix of the accelerometer regarding the robot, $'R_{acc0}$ the rotation matrix between the robot and the accelerometer in the reference position of the arm and $'P_s$ the shoulder joint position regarding the robot. Therefore, the correct elbow position is the one which the Z axis of the ${}^{acc0}R_{acc}^{(i)}$ points the same direction as the cross product between the segment \overline{EW} and

\overline{ES} being S, E and W the shoulder, elbow and wrist joint position.

Finally, the elbow location regarding the robot is estimated as

$$'T_e = \begin{bmatrix} {}^r R_e & {}^r P_e \\ 0 & 1 \end{bmatrix}, \text{ with}$$

$$'R_e = {}^r R_{acc0} \cdot {}^{acc0}R_{acc} \cdot {}^{acc0}R_e$$

being ${}^{acc0}R_e$ the rotation matrix of the elbow regarding the accelerometer in the reference arm position. Once the location of the elbow joint is estimated, the swivel angle, necessary to compute the augmented Jacobian, can be computed [37].

Initial conditions

The initial upper limb joints are necessary to the kinematic reconstruction algorithm. The following locations with respect to the robot are initially known: the shoulder $'T_s$, obtained at the beginning of the therapy; the wrist $'T_w$, known through the end effector of the robot; and the elbow $'T_e$, estimated as explained in the previous section. Thus, the initial joint angles can be estimated using the DH parameters [39] shown in Table 1.

The known matrix that determines the shoulder movement regarding its joints (q_1, q_2, q_3) is defined as

$$'T_s = {}^{s0}T_{s3} = {}^{s0}T_{s1} \cdot {}^{s1}T_{s2} \cdot {}^{s2}T_{s3} \simeq \begin{bmatrix} n_x & n_y & n_z & p_x \\ o_x & o_y & o_z & p_y \\ a_x & a_y & a_z & p_z \\ 0 & 0 & 0 & 1 \end{bmatrix};$$

and two possible solutions of the shoulder joints are obtained as

| | |
|---|--|
| (i) if $q_2 \in [0 \quad \pi]$: | (ii) if $q_2 \in [0 \quad \pi]$: |
| $q_1 = \text{atan2}(-n_y, o_y)$ | $q_1 = \text{atan2}(-n_y, o_y)$ |
| $q_2 = \text{atan2}(a_y, \sqrt{n_y^2 + o_y^2})$ | $q_2 = \text{atan2}(a_y, -\sqrt{n_y^2 + o_y^2})$ |
| $q_3 = \text{atan2}(a_z, -a_x)$ | $q_3 = \text{atan2}(-a_z, a_x)$ |

On the other hand, the flexion-extension of the elbow, joint q_4 , affects the distance \overline{SW} and, therefore, it can be unequivocally computed through the law of the cosines as

$$q_4 = \arcsin \left(\frac{l_u^2 + l_f^2 - ||W - S||^2}{2l_u l_f} \right).$$

Finally, since the wrist location is given by the robot end-effector pose, its transformation matrix $'T_w = {}^{s0}T_{s7}$ is known. Thus, the wrist joints can be also estimated following the criterion used to solve the shoulder joints as

$${}^{s4}T_{s7} = ({}^{s0}T_{s3} \cdot {}^{s3}T_{s4})^{-1} \cdot {}^{s0}T_{s7} \simeq \begin{bmatrix} n_x & n_y & n_z & p_x \\ o_x & o_y & o_z & p_y \\ a_x & a_y & a_z & p_z \\ 0 & 0 & 0 & 1 \end{bmatrix};$$

with $s_3 T_{s_4}$ the homogeneous matrix of the joint q_4 , and two possible solutions can be also obtained as

(iii) if $q_6 \in [-\pi/2, \pi/2]$: (iv) if $q_6 \in [\pi/2, 3\pi/2]$:

$$\begin{array}{ll} q_5 = -\text{atan2}(n_y, o_y) & q_5 = \pi - \text{atan2}(n_y, o_y) \\ q_6 = \arcsin(a_y) & q_6 = \pi - \arcsin(a_y) \\ q_7 = -\text{atan2}(a_x, a_z) & q_7 = \pi - \text{atan2}(a_x, a_z) \end{array}$$

Thereby, four solutions, two due to the shoulder joints and two due to the wrist joints, can satisfy the kinematic constraints. However, only one solution accomplishes the anatomical features of the human upper limb. This statement is provable because the human arm joints vary in $[-\pi/2, \pi/2]$ and each solution belongs either $[0, \pi]$ range or $[0, -\pi]$ range and, therefore, the initial arm joints remain defined. An extensive explanation of the estimation of the initial conditions is presented in Additional file 2.

Experimental protocol

Two different experiments were performed, in the first experiment was intended to measure the accuracy of the proposed algorithm with respect to an optoelectronic system, taken as a ground truth, and the second was intended to study the behaviour of the algorithm in a rehabilitation therapy and compare its stability with respect to the previous algorithm presented in [32]. Data recordings have been approved by the ethics committee of the Miguel Hernández University of Elche, Spain. All the subjects provided written informed consent.

The first experimental exercise was carried out by seven right-handed healthy subjects performing three trials, their main information is presented in Table 2. The subjects wore a specific jacket with 25 markers attached to it using the baseline upper body marker set [40] in order to measure the ‘ground truth’ joints. Thus, the location of the upper arm, forearm and hand were directly obtained through the optoelectronic system and therefore the arm joints were computed as explained in the previous section. In order to estimate the upper limb joints through the proposed algorithm, a magneto-inertial sensor was tightly attached to the upper arm and the wrist joint location

was obtained with the end-effector robot with seven DoF, designed and built by the Neuro-Bioengineering Research Group (nBio), Miguel Hernández University of Elche, Spain [33]. The shoulder joint location was only measured at the beginning of the experimentation through the optoelectronic system as the shoulder and the trunk are fixed during the exercise. The trajectory was previously established in the end-effector robot, a point to point task.

The second experimental exercise was carried out by three post-stroke patients, the scores of two assessment scales are shown in Table 3, Ashworth [41], for the elbow joint, and Fugl-Meyer [42]. Two magneto-inertial sensors were used, one attached to the upper arm and the other onto the shoulder (see Fig. 5). The wrist joints location was computed during the exercise with the end-effector robot called ‘PUPArm’, designed and built by the Neuro-Bioengineering Research Group (nBio), Miguel Hernández University of Elche, Spain; and the shoulder joint location, as the flexion-extension and ulnar-radial deviation of the wrist joint is fixed by the robot, the algorithm proposed in [34] can be used and the shoulder location remains estimated during the exercise. The subjects performed three movements in the roulette activity [43].

In both exercises, the length of the upper arm was manually measured from the lateral side of the acromion to the proximal radius head, in the elbow joint; and the forearm length was measured from the proximal radius head to the radial styloid, the distal part of the radius [44]. Furthermore, the upper limb joints were on-line estimated. The main parameters of the kinematic reconstruction algorithm, the gain matrix and the damping factor, were set to $K = \text{diag}\{1.5, 1.5, \dots, 1.5\} \text{ N/ms}$ and $k^2 = 0.5$ respectively. They were chosen through a “trial and error” approach under the exercise conditions. The magneto-inertial sensors used were developed by Shimmer® and sampled at 100Hz. The optoelectronic system was composed by 8 6DoF optical tracking cameras Optitrack V100: R2, developed by NaturalPoint®. This camera has a $640 \times 480 \text{ px}$ resolution with an approximate precision of 0.3 mm and frame rate of 30 – 120 frames per second.

Results

Validation of the proposed algorithm

This algorithm was previously studied in a simulated environment with a 7 DoF robot, being able to avoid shoulder movements and misalignment between the accelerometer and the upper arm, in [45]. The accuracy of the proposed algorithm was measured as the difference between the values acquired through the optoelectronic system and estimated by the proposed algorithm in terms of Root Mean Square Error (RMSE), Standard Deviation (SD) and correlation coefficient (R), shown in Table 4. It can be observed that the correlation between both upper limb joints reconstruction is high with low error. In addition,

Table 2 Main information of the healthy subjects

| ID | Age | Forearm length [m] | Upper arm length [m] |
|----|-----|--------------------|----------------------|
| 1 | 24 | 0.25 | 0.34 |
| 2 | 31 | 0.21 | 0.30 |
| 3 | 24 | 0.26 | 0.32 |
| 4 | 26 | 0.26 | 0.29 |
| 5 | 29 | 0.26 | 0.31 |
| 6 | 24 | 0.23 | 0.33 |
| 7 | 25 | 0.26 | 0.30 |

Table 3 Main information of the post-stroke patients

| ID | Affected arm | Age | Forearm length [m] | Upper arm length [m] | Fugl-Meyer (A+B+C+D)* | Ashworth |
|----|--------------|-----|--------------------|----------------------|-----------------------|----------|
| 1 | Right | 51 | 0.24 | 0.30 | (33+7+7+2) /66 | 2 |
| 2 | Left | 58 | 0.25 | 0.33 | (27+4+3+3) /66 | 3 |
| 3 | Left | 74 | 0.24 | 0.35 | (24+2+2+1) /66 | 3 |

*Fugl Meyer scale for upper extremity is divided in: A) Upper Extremity, B) Wrist, C) Hand, D) Coordination/speed

the reconstructed kinematic joints of a subject while performing a trial is shown in Fig. 6.

Experimental results with patients

The proposed kinematic reconstruction algorithm was tested in a clinic environment with post-stroke patients during a robot-aided neuro-rehabilitation therapy with the 'PUPArm' robot. In addition, the previous algorithm presented by Papaleo et al. was also studied [32]. Figure 7 shows the upper limb joints estimated with the proposed algorithm and with the previous algorithm. Furthermore, the shoulder displacement of the patients and the trajectory followed with the end effector of the robot are also shown. The gray area denote the instability of the previous algorithm, i.e. the time in which the upper limb joints cannot be estimated with the previous algorithm. In these areas the arm joints were set to the last known value estimated through the previous algorithm. The trajectory followed with the end effector of the robot is also shown in the figure together with the eight possible goals of the roulette exercise [43]. In this case the exercise performed was to achieve three goals. It can be observed that the diameter of the roulette is higher in the user one,

15 cm, than in the user two and three, 13 cm and 12 cm respectively, implying higher estimated ROM in joints q1 and q3 (see Table 5), as it was expected due to the high Fugl-Meyer score (see Table 3).

Discussion

The aim of this study was to develop a robust kinematic reconstruction algorithm of the human upper limb joints being able to perform a real-time joint estimation during a neuro-rehabilitation therapy assisted by robots with only one accelerometer placed onto the upper arm. Furthermore, the previous algorithm, presented in [32], the initial upper limb joints; the upper arm and the forearm length; and the shoulder position were measured by the optoelectronic system, not used in a clinical environment. Therefore, we have defined a protocol to manually measure the upper arm and forearm lengths; we have introduced a mathematical method to estimate the initial upper limb joints; and the presented algorithm, as it is based on the computation of the accelerometer rotation, is always able to estimate the upper limb joints.

The kinematic reconstruction algorithm proposed shows high correlation with respect to the real upper arm.

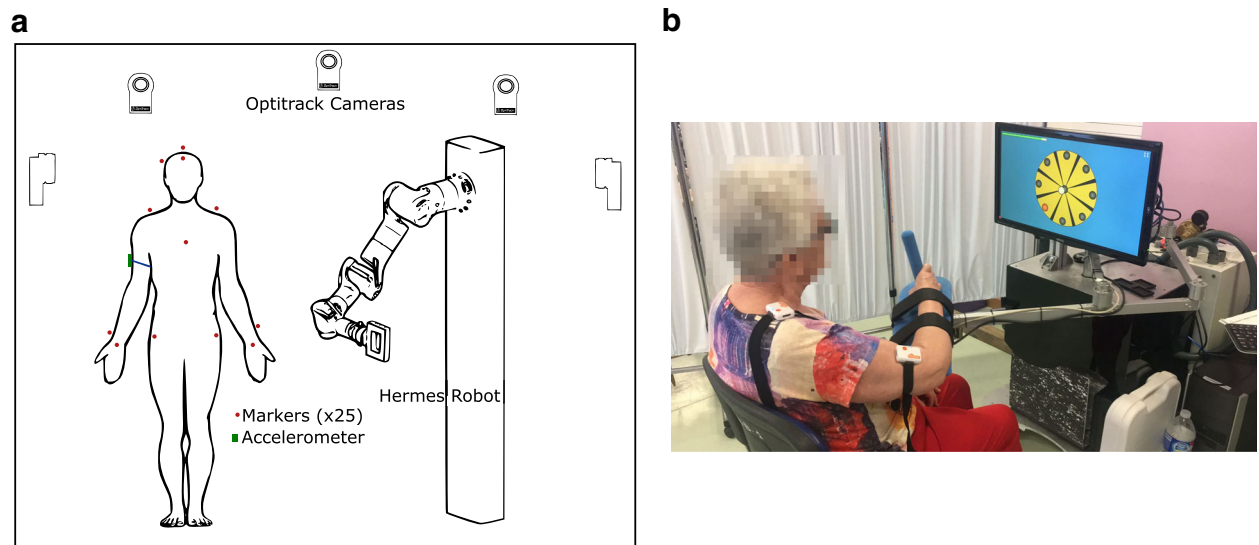


Fig. 5 Experimental exercises. **a** Healthy subjects performed an arm movement using a 7 DoF robot wearing an accelerometer placed onto the upper arm and special jacket with optoelectronic markers. **b** Post-stroke patients performed arm movements using the 'PUPArm' robot wearing an accelerometer placed onto the upper arm and a magneto-inertial device placed onto the shoulder

Table 4 RMSE of the proposed algorithm regarding the optoelectronic system reconstruction (grand mean of the seven subjects)

| | RMSE | SD | R | p-value |
|---------------------------|-------|-------|-------|---------|
| Elbow joint position [cm] | 2.13 | 1.1 | 0.977 | < 0.001 |
| Wrist joint position [cm] | 1.89 | 1.12 | 0.982 | < 0.001 |
| q_1 [deg] | 3.548 | 2.148 | 0.957 | < 0.001 |
| q_2 [deg] | 3.271 | 2.992 | 0.977 | < 0.001 |
| q_3 [deg] | 4.569 | 3.041 | 0.966 | < 0.001 |
| q_4 [deg] | 1.719 | 1.542 | 0.995 | < 0.001 |
| q_5 [deg] | 4.506 | 2.741 | 0.873 | < 0.001 |
| q_6 [deg] | 2.825 | 2.226 | 0.899 | < 0.001 |
| q_7 [deg] | 4.742 | 3.279 | 0.982 | < 0.001 |

Although the error committed in the estimation of the wrist and shoulder position is low, 2 cm approximately, it implies an upper limb joints RMSE about 3.5 degrees (mean of the seven joints) with high correlation in all joints. It must be noticed that q_5 and q_6 joints have low correlation with respect to the others, it may be due to these joints are in the distal part of the arm where the error between the real arm and the estimated arm is maximum and the estimation could differ slightly.

The second experiment was intended to study the behavior of the proposed and previous algorithms in patients during a neuro-rehabilitation therapy assisted by end-effector robots, being able to estimate the shoulder movements using the method proposed in [34] and assuming the joints q_6 and q_7 fixed by the robot. Figure 7 shows that the previous algorithm is unstable when shoulder movements appear, areas marked in gray, whilst the

proposed not. Although the shoulder is assumed fixed in both methods, it is very difficult to fix the shoulder and avoid little displacements with patients. It must be noticed that, before the error appears, the difference between both algorithms increases and, after the instability, the previous algorithm tends to follow the proposed estimated joints. Therefore, we can say that in the areas when the previous algorithm fails the proposed kinematic reconstruction performs a correct estimation. This error appears due to the method employed in the estimation of the elbow joint location because it is based on the strict constrains of the human upper limb which, a little movement of the shoulder assumed fixed, can lead to the algorithm failure. Furthermore, this error is closely related to the ROM estimation, a very important parameter in these therapies, and could lead a false ROM improvement [17]. Therefore, it is very important the stability of the kinematic reconstruction algorithm during the exercise.

On the other hand, the estimation of the ROM together with the assessments scales proposed and the trajectory performed by the user with the end effector of the robot encompasses an objective and comprehensive assessment of the patient condition during a robot-aided neuro-rehabilitation therapy. Thus, it can be observed that subject 3 performed worse trajectories than the other two subjects as it was expected due to the low score on the Fugl-Meyer scale with high Ashworth score. Furthermore, the patient with higher Fugl-Meyer and less Ashworth scores has the highest estimated ROM.

Conclusions

The presented kinematic reconstruction algorithm of the human upper limbs has a low error regarding the real arm acquired through an optoelectronic system. This

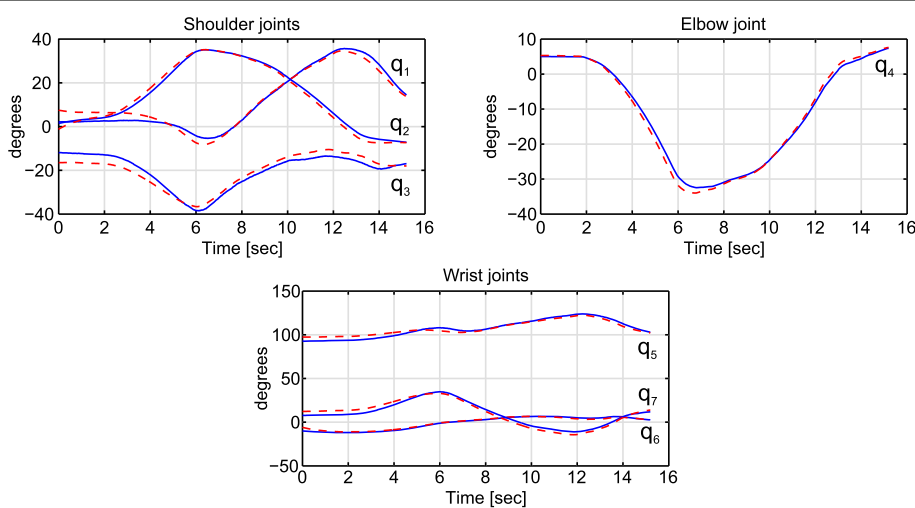


Fig. 6 Reconstructed upper limb joints estimated by the proposed algorithm (blue smooth line) and acquired through the optoelectronic system (red dotted line) of one trial performed by a healthy subject

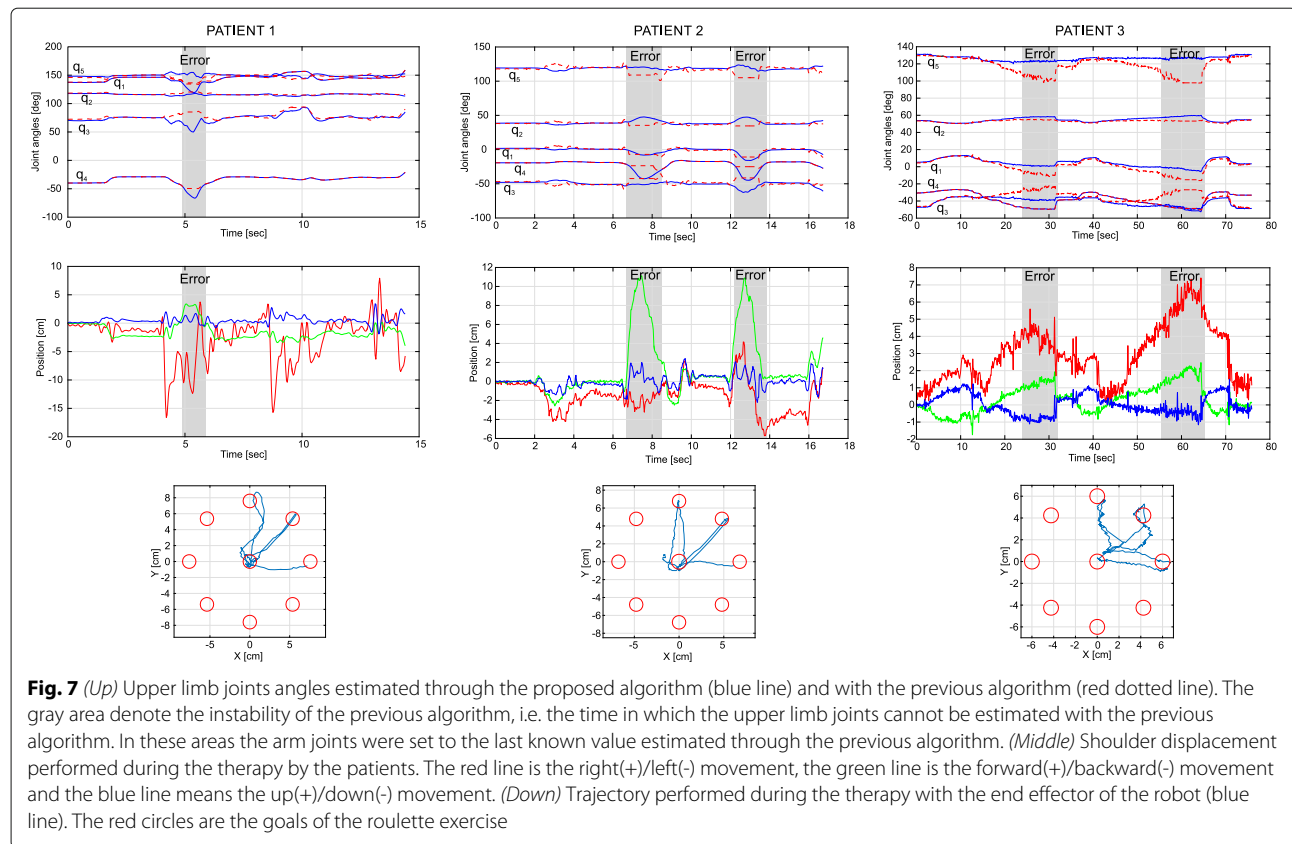


Fig. 7 (Up) Upper limb joints angles estimated through the proposed algorithm (blue line) and with the previous algorithm (red dotted line). The gray area denote the instability of the previous algorithm, i.e. the time in which the upper limb joints cannot be estimated with the previous algorithm. In these areas the arm joints were set to the last known value estimated through the previous algorithm. (Middle) Shoulder displacement performed during the therapy by the patients. The red line is the right(+)/left(-) movement, the green line is the forward(+)/backward(-) movement and the blue line means the up(+)/down(-) movement. (Down) Trajectory performed during the therapy with the end effector of the robot (blue line). The red circles are the goals of the roulette exercise

algorithm performs the kinematic reconstruction during the exercise allowing the therapist to correct, in real time, wrong upper limb position. Furthermore, compared to the previous algorithm, it is stable; proposes a protocol to manually measure the upper arm and forearm length; and estimates the initial upper limb joints being able to be used in a clinic environment. In addition, the study of the kinematics in the ‘normal’ model, performed by healthy subjects, during robot-aided rehabilitation tasks could be directly applied in the evaluation of the patients. Finally, the ROM estimation of the upper limb joints together with the assessment scales, as Fugl-Meyer or Ashworth, and the trajectory performed by the patient allows the therapist to have a comprehensive assessment during the therapy.

Table 5 ROM, in degrees, estimated through the proposed algorithm during the therapy

| ID | Joint q ₁ | Joint q ₂ | Joint q ₃ | Joint q ₄ | Joint q ₅ |
|----|----------------------|----------------------|----------------------|----------------------|----------------------|
| 1 | 37.5 | 5.46 | 43.63 | 35.8 | 11.78 |
| 2 | 17.99 | 11.74 | 18.04 | 29.29 | 9.20 |
| 3 | 18.99 | 9.47 | 16.13 | 26.04 | 11.38 |

Additional files

[Additional file 1:](#) Solution of γ angle. (PDF 104 kb)

[Additional file 2:](#) Estimation of the initial conditions. (PDF 107 kb)

Abbreviations

DH: Denavit-hartenberg; DoF: Degree of freedom; MSE: Root Mean square error; ROM: Range of motion; SD: Standard deviation

Acknowledgements

The authors thank the subjects for their participation. In addition, we acknowledge the great support from Hospital Vega Baja, Orihuela, Alicante, Spain and the Biomedical Research Networking Center (CIBER). Special thanks to the therapist Irene Delegido.

Funding

This work has been supported by the AIDE project through the grant agreement no. 645322 of the European Commission, by the AURORA project through the grant DPI2015-70415-C2-R of the Ministerio de Economía y Competitividad of Spain, by the HOMEREHAB project through the grant agreement no. 601116 of the European Union’s Seventh Framework Programme and by Conselleria d’Educació, Cultura i Esport of Generalitat Valenciana through the grant APOTIP 2017/001.

Availability of data and materials

Data and materials can be made available upon request to the corresponding author.

Authors’ contributions

ABM and FJB conceived of and designed the experiments. ABM and AB performed the experiments. ABM and JAB analyzed the data. ABM drafted the

paper. NGA and LZ deeply revised the manuscript. All the authors checked and approved the final submitted version of the manuscript.

Ethics approval and consent to participate

Data recordings have been approved by the ethics committee of the Miguel Hernández University of Elche, Spain. All the subjects provided written informed consent.

Consent for publication

Not applicable.

Competing interests

The authors declare that they have no competing interests.

Publisher's Note

Springer Nature remains neutral with regard to jurisdictional claims in published maps and institutional affiliations.

Author details

¹Miguel Hernández University of Elche, Av. Universidad w/n, Ed. Innova, 03202 Elche, Spain. ²Universidad de Cadiz, Avenida de la Universidad n 10, 11519 Puerto Real, Spain. ³Research Unit of Biomedical Robotics and Biomicrosystems, Università Campus Bio-Medico di Roma, via Álvaro del Portillo, 21, 00128 Roma, Italy.

Received: 28 July 2017 Accepted: 31 January 2018

Published online: 20 February 2018

References

- Lo AC, et al. Robot-assisted therapy for long-term upper-limb impairment after stroke. *N Engl J Med.* 2010;362(19):1772–83. <https://doi.org/10.1056/NEJMoa0911341>. PMID: 20400552.
- Krebs HI, et al. Rehabilitation robotics: Performance-based progressive robot-assisted therapy. *Autonomous Robots.* 2003;15(1):7–20. <https://doi.org/10.1023/A:1024494031121>.
- Donnan GA, Fisher M, Macleod M, Davis SM. Stroke. *The Lancet.* 2008;371(9624):1612–23. [https://doi.org/10.1016/S0140-6736\(08\)60694-7](https://doi.org/10.1016/S0140-6736(08)60694-7).
- Miller EL, et al. Comprehensive overview of nursing and interdisciplinary rehabilitation care of the stroke patient: A scientific statement from the american heart association. *Stroke.* 2010;41(10):2402–48. <https://doi.org/10.1161/STR.0b013e3181e7512b>.
- Riener R, Nef T, Colombo G. Robot-aided neurorehabilitation of the upper extremities. *Med Biol Eng Comput.* 2005;43(1):2–10. <https://doi.org/10.1007/BF02345116>.
- Novak D, Nagle A, Keller U, Riener R. Increasing motivation in robot-aided arm rehabilitation with competitive and cooperative gameplay. *J NeuroEng Rehabil.* 2014;11(1):64–79. <https://doi.org/10.1186/1743-0003-11-64>.
- Lo HS, Xie SQ. Exoskeleton robots for upper-limb rehabilitation: State of the art and future prospects. *Medical Eng Phys.* 2012;34(3):261–8.
- Chang WH, Kim YH. Robot-assisted therapy in stroke rehabilitation. *J stroke.* 2013;15(3):174.
- Vitiello N, Lenzi T, Roccella S, De Rossi SMM, Cattin E, Giovacchini F, Vecchi F, Carrozza MC. Neuroexos: A powered elbow exoskeleton for physical rehabilitation. *IEEE Trans Robot.* 2013;29(1):220–35. <https://doi.org/10.1109/TRO.2012.2211492>.
- Lenzi T, De Rossi SMM, Vitiello N, Carrozza MC. Intention-based emg control for powered exoskeletons. *Trans Biomed Eng.* 2012;59(8):2180–90. <https://doi.org/10.1109/TBME.2012.2198821>.
- Burgar CG, Lum PS, Shor PC, Van der Loos HM. Development of robots for rehabilitation therapy: the palo alto va/stanford experience. *J Rehab Res Dev.* 2000;37(6):663–74.
- Krebs HI, Volpe BT, Ferraro M, Fasoli S, Palazzolo J, Rohrer B, Edelstein L, Hogan N. Robot-aided neurorehabilitation: from evidence-based to science-based rehabilitation. *Top Stroke Rehabil.* 2002;8(4):54–70.
- Reinkensmeyer DJ, Kahn LE, Averbuch M, McKenna-Cole A, et al. Understanding and treating arm movement impairment after chronic brain injury: progress with the arm guide. *J Rehab Res Dev.* 2000;37(6):653.
- Coote S, Stokes E, Murphy B, Harwin W. The effect of GENTLE/S robot-mediated therapy on upper extremity dysfunction post stroke. *Proceedings of the 8th International Conference on Rehabilitation Robotics.* 2003, pp. 23–5.
- Zollo L, Rossini L, Bravi M, Magrone G, Sterzi S, Guglielmelli E. Quantitative evaluation of upper-limb motor control in robot-aided rehabilitation. *Med Biol Eng Comput.* 2011;49(10):1131.
- de los Reyes-Guzmán A, Dimbwadyo-Terrer I, Trincado-Alonso F, Monasterio-Huelin F, Torricelli D, Gil-Aguado A. Quantitative assessment based on kinematic measures of functional impairments during upper extremity movements: A review. *Clin Biomech.* 2014;29(7):719–27.
- Nordin N, Xie SQ, Wünsche B. Assessment of movement quality in robot-assisted upper limb rehabilitation after stroke: a review. *J Neuroengineering Rehab.* 2014;11(1):137.
- Lum PS, Burgar CG, Shor PC, Majmundar M, Van der Loos M. Robot-assisted movement training compared with conventional therapy techniques for the rehabilitation of upper-limb motor function after stroke. *Arch Phys Med Rehabil.* 2002;83(7):952–9.
- Winstein CJ, Rose DK, Tan SM, Lewthwaite R, Chui HC, Azen SP. A randomized controlled comparison of upper-extremity rehabilitation strategies in acute stroke: a pilot study of immediate and long-term outcomes. *Arch Phys Med Rehabil.* 2004;85(4):620–8.
- Kwakkel G, Kollen BJ, Krebs HI. Effects of robot-assisted therapy on upper limb recovery after stroke: A systematic review. *Neurorehabil Neural Repair.* 2007. <https://doi.org/10.1177/1545968307305457>.
- Kirk AG, O'Brien JF, Forsyth DA. Skeletal parameter estimation from optical motion capture data. *2005 IEEE Computer Society Conference on Computer Vision and Pattern Recognition (CVPR'05).* 2005;2:782–8. <https://doi.org/10.1109/CVPR.2005.326>.
- Tognetti A, Lorusso F, Carbonaro N, De Rossi D. Wearable goniometer and accelerometer sensory fusion for knee joint angle measurement in daily life. *Sensors.* 2015;15(11):28435–55.
- Stupar DZ, Bajic JS, Manojlovic LM, Slankamenac MP, Joza AV, Zivanov MB. Wearable low-cost system for human joint movements monitoring based on fiber-optic curvature sensor. *IEEE Sensors J.* 2012;12(12):3424–31.
- Mengüç Y, Park YL, Pei H, Vogt D, Aubin PM, Winchell E, Fluke L, Stirling L, Wood RJ, Walsh CJ. Wearable soft sensing suit for human gait measurement. *Int J Robot Res.* 2014;33(14):1748–64.
- Leardini A, Lullini G, Giannini S, Bertì L, Ortolani M, Caravaggi P. Validation of the angular measurements of a new inertial-measurement-unit based rehabilitation system: comparison with state-of-the-art gait analysis. *J Neuroengineering Rehab.* 2014;11(1):136.
- Seel T, Raisch J, Schauer T. Imu-based joint angle measurement for gait analysis. *Sensors.* 2014;14(4):6891–909.
- Roetenberg D, Luinge H, Slycke P. Xsens mvn: full 6dof human motion tracking using miniature inertial sensors. *Xsens Motion Technologies BV, Tech. Rep.* 2009.
- Novak D, Goršič M, Podobnik J, Munih M. Toward real-time automated detection of turns during gait using wearable inertial measurement units. *Sensors.* 2014;14(10):18800–22. <https://doi.org/10.3390/s141018800>.
- Klopčar N, Lenarčič J. Kinematic model for determination of human arm reachable workspace. *Meccanica.* 2005;40(2):203–19. <https://doi.org/10.1007/s11012-005-3067-0>.
- Cameirão M, Badia S, Oller E, Verschure P. Neurorehabilitation using the virtual reality based rehabilitation gaming system: methodology, design, psychometrics, usability and validation. *J NeuroEng Rehab.* 2010;7(1):48–62. <http://doi.org/10.1186/1743-0003-7-48>.
- Mihelj M. Human arm kinematics for robot based rehabilitation. *Robotica.* 2006;24(3):377–83. <https://doi.org/10.1017/S0263574705002304>.
- Papaleo E, et al. Upper-limb kinematic reconstruction during stroke robot-aided therapy. *Med Biol Eng Comput.* 2015;53(9):815–28. <https://doi.org/10.1007/s11517-015-1276-9>.
- Badesa FJ, Morales R, Garcia-Aracil N, Sabater JM, Perez-Vidal C, Fernandez E. Multimodal interfaces to improve therapeutic outcomes in robot-assisted rehabilitation. *IEEE T Syst Man Cy C.* 2012;42(6):1152–8. <https://doi.org/10.1109/TSMC.2012.2201938>.
- Bertomeu-Motos A, Lledó LD, Diez JA, Catalán JM, Ezquerro S, Badesa FJ, Garcia-Aracil N. Estimation of human arm joints using two wireless sensors in robotic rehabilitation tasks. *Sensors.* 2015;15(12):30571–83. <https://doi.org/10.3390/s151229818>.
- Lenarčič J, Umek A. Simple model of human arm reachable workspace. *IEEE T Syst Man Cyb.* 1994;24(8):1239–46. <https://doi.org/10.1109/21.299704>.

36. Denavit J. A kinematic notation for lower-pair mechanisms based on matrices. *J Appl Mech, ASME*. 1955;22:215–21.
37. Kreutz-Delgado K, Long M, Seraji H. Kinematic analysis of 7 dof anthropomorphic arms. In: Proc 1990 IEEE Int Conf Robot Autom. p. 824–30. <https://doi.org/10.1109/ROBOT.1990.126090>.
38. Siciliano B. Kinematic control of redundant robot manipulators: A tutorial. *J Intell Robot Syst*. 1990;3(3):201–12. <https://doi.org/10.1007/BF00126069>.
39. Siciliano B, Sciacicco L, Villani L, Oriolo G. Robotics: Modelling, Planning and Control. London: Springer-Verlag; 2009. <https://doi.org/10.1007/978-1-84628-642-1>.
40. Baseline Upper Body (25) Markerset. [https://v20.wiki.optitrack.com/index.php?title=Baseline_Upper_Body_\(25\)](https://v20.wiki.optitrack.com/index.php?title=Baseline_Upper_Body_(25)). Accessed 28 Nov 2017.
41. Charalambous CP. Interrater reliability of a modified ashworth scale of muscle spasticity. Classic Papers in Orthopaedics. London: Springer; 2014, pp. 415–7. https://doi.org/10.1007/978-1-4471-5451-8_105.
42. Fugl-Meyer AR, Jääskö L, Leyman I, Olsson S, Steglind S. The post-stroke hemiplegic patient. 1. a method for evaluation of physical performance. *Scand J Rehabil Med*. 1975;7(1):13–31.
43. Lledo LD, Diez JA, Bertomeu-Motos A, Ezquerro S, Badesa FJ, Sabater-Navarro JM, Garcia-Aracil N. A comparative analysis of 2d and 3d tasks for virtual reality therapies based on robotic-assisted. *Front Aging Neurosci*. 2016;8:205. <https://doi.org/10.3389/fnagi.2016.00205>.
44. Mazza JC. Mediciones antropométricas. estandarización de las técnicas de medición, actualizada según parámetros internacionales. *Revista de Actualización en Ciencias del Deporte*. 1993;1(2):197.
45. Bertomeu-Motos A, Morales R, Lledó LD, Diez JA, Catalan JM, Garcia-Aracil N. Kinematic reconstruction of the human arm joints in robot-aided therapies with hermes robot. In: 2015 37th Annual International Conference of the IEEE Engineering in Medicine and Biology Society (EMBC). 2015. p. 1190–3. <https://doi.org/10.1109/EMBC.2015.7318579>.

Submit your next manuscript to BioMed Central and we will help you at every step:

- We accept pre-submission inquiries
- Our selector tool helps you to find the most relevant journal
- We provide round the clock customer support
- Convenient online submission
- Thorough peer review
- Inclusion in PubMed and all major indexing services
- Maximum visibility for your research

Submit your manuscript at
www.biomedcentral.com/submit

